SCIENCE CHINA
Information Sciences

• **Supplementary File** •

Proximity-Induced Magnetic Order in Topological Insulator on Ferromagnetic Semiconductor

Hangtian Wang[1,2], Koichi Murata[3], Weiran Xie[1], Jing Li[1], Jie Zhang[1*], Kang L. Wang[3], Weisheng Zhao[1,2] & Tianxiao Nie[1,2*]

[1]*School of Integrated Circuit Science and Engineering and Advanced Innovation Center for Big Data and Brain Computing, Beihang University, Beijing* 100191*, China;*
[2]*Beihang-Goertek Joint Microelectronics Institute, Qingdao Research Institute, Beihang University, Qingdao* 266000*, China;*
[3] *Department of Electrical Engineering, University of California, Los Angeles, California* 90095*, USA*

Appendix A TEM images of Ge-Se grain and Bi_2Se_3 crystal

During the heterostructure preparation, the growth temperature of the substrate must be strictly kept at 200℃. Above it, a Se-Ge impurity phase will be easily formed instead of Bi_2Se_3, which could be verified by TEM results in Figure A1. Figure A1(a) shows two separated Ge-Se grains on Mn_xGe_{1-x}, the size of these grains is approximately 100 nm. No obvious connection was observed between the two grains, demonstrating the island growth mode of Ge-Se. Figure A1(b) is the corresponding zoom-in TEM image of the Ge-Se grain. On the contrary, Bi_2Se_3 film shows a perfect crystallinity due to its 2D growth mode, as shown in Figure A1(c).

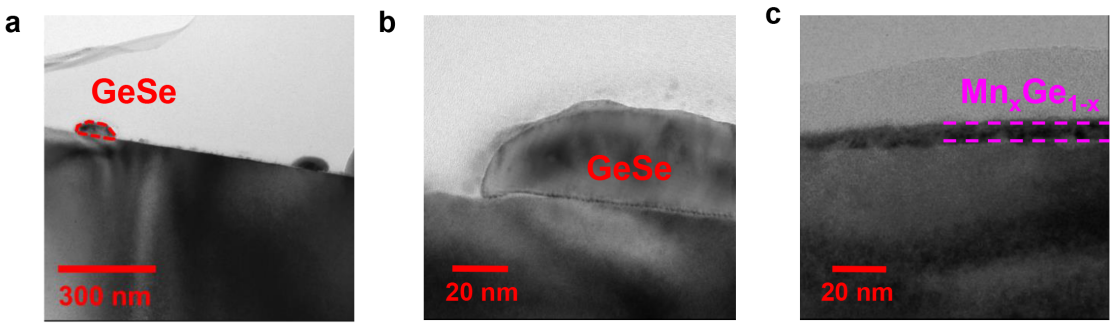

Figure A1 TEM images of Ge-Se grain and Bi_2Se_3 crystal. (a) TEM images of the Ge-Se impurity phase on Mn_xGe_{1-x}. (b) A magnified TEM image of the crystal structure of Ge-Se grains. (c) TEM images of pure Bi_2Se_3 on Mn_xGe_{1-x}. A flat surface morphology and sharp Mn_xGe_{1-x}/Bi_2Se_3 interface can be clearly observed.

Appendix B Transport measurements for pure Mn_xGe_{1-x} (x=0.04)

To exclude the contribution of the Mn_xGe_{1-x} conductance channels on the heterostructure, a 20 nm Mn_xGe_{1-x} (x=0.04) film was prepared with the same growth condition as the heterostructure for the transport measurement. The temperature-dependent Hall curves of Mn_xGe_{1-x} are shown in Figure A2(a). A clear magnetic hysteresis loop could be observed up to 150 K. As the temperature continuously increases, the hysteresis loop gradually degrades, which indicates that the Mn_xGe_{1-x} thin film goes through a transition from a ferromagnetic to a paramagnetic state at 150 K-200 K. The same conclusion could be obtained in Figure A2(b), the MR of Mn_xGe_{1-x} thin film shows a negative behavior from 1.9 K-150K, indicating that the T_c of Mn_xGe_{1-x} is around 150 K. By contrast, no hysteresis loop is observed in pure Bi_2Se_3 even at 1.9 K, as shown in the inset in Figure A2(a). Notably, the MR of Mn_xGe_{1-x} (0.1% at 1T) is much smaller than that of the Bi_2Se_3/Mn_xGe_{1-x} heterostructure (2% at 1T, Figure 2f), which proves that the Mn_xGe_{1-x} conductance is almost negligible for the transport channels in the heterostructure.

* Corresponding author (email: zhangjie2019@buaa.edu.cn, nietianxiao@buaa.edu.cn)
† Hangtian Wang and Weiran Xie have the same contribution to this work.

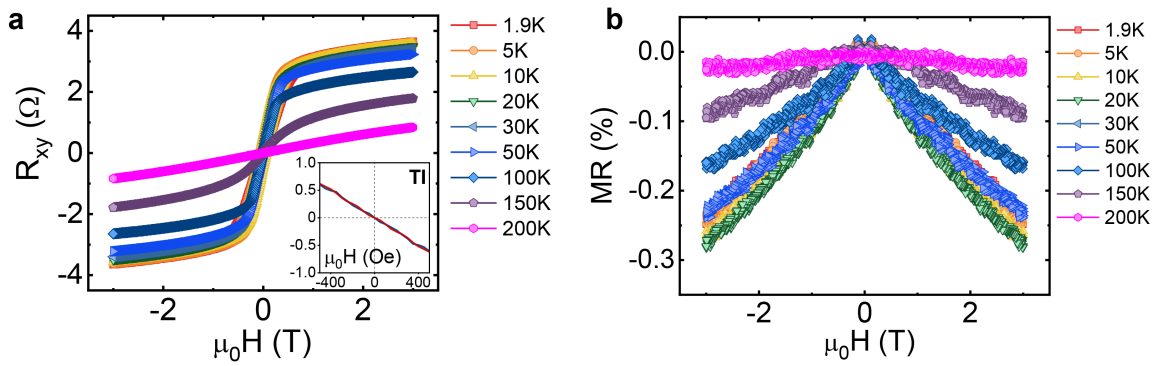

Figure B1 Transport measurements for pure Mn_xGe_{1-x} (x=0.04). (a) The temperature-dependent Hall and (b) MR curves. Inset: the Hall curve for pure Bi_2Se_3 at 1.9K

Appendix C Transport measurements for pure Bi_2Se_3 and the heterostructure

To analyze the quantum corrections to conductivity from WL and WAL, the temperature-dependent resistance and conductivity of pure Bi_2Se_3 and the heterostructure are extracted in Figure A3. Figure A3(a) describes the resistance-temperature (R-T) curve for Bi_2Se_3 film. The plateau from 1.9 K-10 K results from the freezing of the bulk carriers in Bi_2Se_3. After converting it to a conductivity plot (Figure A3(c)), a logarithmic conductivity increase can be observed, which comes from the quantum correction by WAL and EEI in the surface states. In the heterostructure, the same logarithmic increase can be noticed, as shown in Figure A3(b) and A3(d), which results from the combined effect of quantum corrections induced by WAL, WL, and EEI effects.

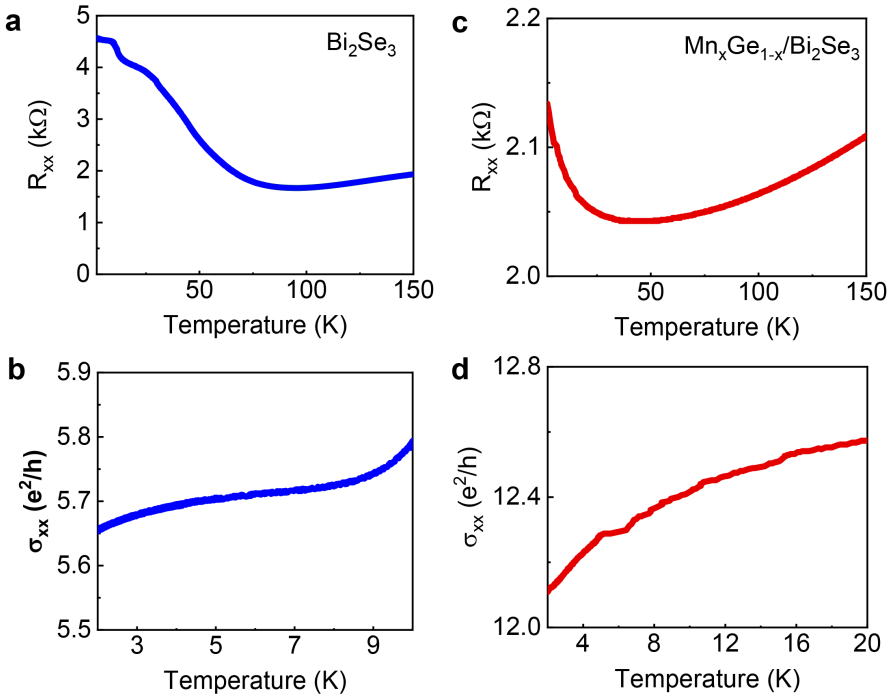

Figure C1 Transport measurements for pure Bi_2Se_3 and the heterostructure. (a, b) R-T curves for two samples. (c, d) The quantum correction induced logarithmic conductivities increase in low-temperature regions.

Appendix D Estimation of the surface state gap size

In the heterostructure, both the WAL prefactor α_1 and WL prefactor α_2 in the quantum interferences are related to the band gap in the surface states and the Fermi level E_F. Specifically, α_1 and α_2 can be expressed as [1]:

$$\alpha_1 = -\frac{a^4b^4}{(a^4+b^4)(a^4+b^4-a^2b^2)} \tag{D1}$$

$$\alpha_2 = \frac{(a^4+b^4)(a^2-b^2)^2}{2(a^4+b^4-a^2b^2)^2} \tag{D2}$$

Here $a \equiv \cos\frac{\Theta}{2}$, $b \equiv \sin\frac{\Theta}{2}$, and $\cos\Theta \equiv \frac{\Delta}{2E_F}$. Obviously, either α_1 or α_2 is determined by the bandgap size (Δ). In topological surface states, the band is gapless with $\cos\Theta \to 0$, then the conductance channel is dominated by the WAL effect with α_1=-1/2 and α_2=0. By contrast, if a surface state gap is opened by magnetism, and the Fermi level locates in the gap ($\cos\Theta \to 1$), the quantum correction can be driven into the WL regime with α_1=0 and α_2=1/2. In addition, the Fermi level position relative to the Dirac point E_F can be estimated by the formula [2]:

$$E_F = \hbar/(2m^*)(3\pi N_{BD})^{2/3} \tag{D3}$$

Here the effective mass m^* is assumed to be $m^* \approx 0.15m_e$, and the bulk carrier density N_{BD} at 1.9 K can be extracted as $9.4 \times 10^{18}\,\mathrm{cm}^{-3}$ from Figure 2d. Therefore, the E_F of Bi_2Se_3 in the heterostructure is fixed approximately at ∼0.113 eV. Finally, by using the value of E_F and the obtained α_1, α_2 in Figure 4a, the surface state bandgap of the Bi_2Se_3 layer is estimated to be $\Delta \approx 80$ meV at 1.9 K.

References

1 ALu H-Z, Shi J, Shen S-Q. Competition between Weak Localization and Antilocalization in Topological Surface States. Phys Rev Lett, 2011, 107: 076801

2 Brahlek M, Koirala N, Bansal N, et al. Transport properties of topological insulators: Band bending, bulk metal-to-insulator transition, and weak anti-localization. Solid State Commun, 2015, 215-216: 54-62